Biochimica et Biophysica Acta, 1144 (1993) 331–345

BBABIO 43888

Chemical reduction of the water splitting enzyme system of photosynthesis and its light-induced reoxidation characterized by optical and mass spectrometric measurements: A basis for the estimation of the states of the redox active manganese and of water in the quaternary oxygen-evolving S-state cycle

H. Kretschmann and H.T. Witt

Max-Volmer-Institut für Biophysikalische und Physikalische Chemie, Technische Universität Berlin, Berlin (Germany)

(Received 12 March 1992)
(Revised manuscript received 31 March 1993)

Key words: Oxygen evolution; Hydroxylamine; Hydrazine; S state; Absorption change; Mass spectrometry; (*Synechococcus* sp.)

The chemical reduction and over-reduction of the water-splitting enzyme and its subsequent light-induced reoxidation was followed by simultaneous measurements of (i) UV and (ii) electrochromic absorption changes, accompanied (iii) by O_2 measurement and (iv) mass spectrometric analysis of the evolved $^{15}N_2$ and $^{15}N_2O$ of the applied reductant, $^{15}NH_2OH$. (1) On this reversible pathway, the measured four characteristics attributed to changes of Mn valences, surplus charges, water oxidation and oxidation of the reductant are quantitatively coupled with each other. (2) Treatment with NH_2OH (or NH_2NH_2) leads to a three-digit reverse shift of O_2 evolution and UV and electrochromic absorption changes. This is interpreted as the reduction of the enzyme in the dark from the S_1 state via the S_0 and the overreduced S_{-1} state to the superreduced state, S_{-2}. (3) S_{-2} is stable for hours. (4) S_{-2} is a terminal state, not further reducible without being deactivated. (5) Each step on this reversible pathway from state S_1 to S_{-2} is accompanied by a $1/2$-$^{15}N_2$ evolution from $^{15}NH_2OH$ interpreted as a three-electron reduction of state S_1 which is in accordance with the three-digit reverse shifts. (6) The results are explained by a reversible reduction of 3 redox-active Mn ions. Based on the obtained data, the possible valence states of these photooxidizable Mn ions in state S_{-2} to S_3 have been estimated. (7) Irreversible deactivation of S_{-2} with release of Mn into the solution is coupled with an approx. 1-$^{15}N_2O$ evolution from $^{15}NH_2OH$. (8) The electrochromic changes indicate at pH 7 a surplus charge at S_{-1}, S_2 and S_3. This is explained by an H^+ release of approx. 2:1:0:1 with the 1:1:1:1 electron extraction in the $S_{-1} \rightarrow S_0 \rightarrow S_1 \rightarrow S_2 \rightarrow S_3$ transition. On this basis, the possible states of the water derivatives up to S_3 have been estimated. (9) The results are compared with information obtained from UV-difference spectra and XAS, EPR and NMR measurements.

Introduction

After light excitation in reaction center II of photosynthesis a primary stable transmembrane charge separation takes place [1] between Chl a_{II}(P680) [2,3] and the special plastoquinone, Q_A [4,37]. The redox potential of Chl a_{II}^+/Chl a_{II} is the water-splitting motive force. Chl a_{II}^+ oxidizes the immediate donor tyrosine [5–7] which, in turn, extracts an electron out of the water-splitting complex; after four such turnovers the complex is oxidized from state S_0 to states $S_1 \rightarrow S_4$. The subscripts indicate the number of electrons extracted from the complex. O_2 is released in the transition from S_4 to S_0 [8,9]. After dark adaptation, S_1 is the most stable state. Therefore, the transition in a train of flashes starts with $S_1 \rightarrow S_2 \rightarrow S_3 \rightarrow (S_4) \rightarrow S_0$, etc. Thereby, the O_2-evolution maximum occurs upon the 3rd, 7th, 11th, etc., flash.

UV absorption changes coupled with the S-state oxidation have been attributed to changes of the oxidation states of manganese [10–12]. Electrochromic absorption changes have been attributed to the creation of surplus charges ⊕ in the S_2 and S_3 state and to corresponding proton releases from the S states, respectively [13,14]. The surplus charges were independently documented through a strong retardation of the

Correspondence to: H.T. Witt, Max-Volmer-Institut für Biophysikalische und Physikalische Chemie, Technische Universität Berlin, Straße des 17. Juni 135, D-1000 Berlin 12, Germany.

Abbreviations: Chl, chlorophyll; HA, NH_2OH; HH, NH_2NH_2; HA or HH, NH_2R; MS, mass spectrometry; OEC, O_2-evolving complex; Sol, solution; XAS, X-ray absorption spectrometry; DCBQ, 2,5-dichloro-*p*-benzoquinone; FeCy, $K_3[Fe(CN)_6]$; PPBQ, phenyl-*p*-benzoquinone.

electron transfer times from S_2 and S_3, respectively, to Chl a_{II}^+ in comparison with the times of the transfer from S_0 and S_1, respectively [15].

In the presence of the reducing agents hydroxylamine (HA) and hydrazine (HH), a backward shift of the S-state transitions by 2 states was observed; i.e., 5 flashes instead of 3 were required to reach maximum O_2 evolution [16,17]. The two-digit delay is observed in the pattern of UV and electrochromic changes as well [18]. The S-state transitions therefore start with a formal new state, S_{-1}; i.e., the sequence is $S_{-1} \rightarrow S_0 \rightarrow S_1 \rightarrow S_2 \rightarrow S_3 \rightarrow (S_4) \rightarrow S_0$. We have outlined that the nature of the S_{-1} state is of great interest, because it may be a possible basis for the estimation of the properties of the S_0–S_4 states.

It has been discussed that HA is reversibly bound to S_1 (i.e., S_{-1} should be, e.g., $S_1 \cdot n \cdot HA$) so that the two-digit flash delay is realized by a reduction of $S_2 \cdot n \cdot HA$ to S_0 after the 1st flash [19]. Two other models have been proposed [16,20], including reductions of unknown intermediates between the S states and HA [21]. In all models the shift was explained by a combination of different dark reactions before or/after the flashes, but thereby all considered only the native states S_0, S_1 and S_2.

(1) We have proposed that a two-electron reduction of S_1 by HA takes place in the dark via S_0 to a new over-reduced state, S_{-1}, through the reduction of manganese, Mn [18,11]. This was predicted because with the two-digit shift, a new UV-absorption change attributed to Mn as well as new electrochromic changes were observed beyond the S_0 state [18]. We suggested that Mn ions are reduced by HA to the lowest level, i.e., to the Mn(II) states. Considering only two redox-active Mn ions, the terminal state of these should be S_{-1} (2 Mn(II)). On this basis, the possible valences of these two Mn for S_0–S_3 were estimated. The UV-difference spectra are in line with these valences insofar as the spectrum of the $S_0 \rightarrow S_1$ transition is different from the similar spectra of the $S_1 \rightarrow S_2$ and $S_2 \rightarrow S_3$ transitions [11].

(2) Beck and Brudvig have presented evidence for a chemical dark reaction of HA with the S_1 state, following the multiline EPR signal [22], but with different conclusions (see Discussion). In continuation of this program, further evidence for a dark-reduction of S through HA was provided in two ways.

(3) After effective removal of the unreacted HA, the two-state delay of oxygen evolution and also that of the Mn oxidation and formation of surplus charges remains effective, even after 10 h [23].

(4) In the case of a dark reduction of S_1 by a one-electron donor such as HA, the two-state delay of O_2 evolution should not depend on the previous ratio of S_0/S_1. We have shown with reaction center II complexes from cyanobacteria that in the presence of HA a two-digit shift of the S states takes place, independent of the previous S_0/S_{-1} ratio [24]. In addition, after much stronger treatment with HA, a three-digit shift and maximum O_2 evolution in the 6th flash became visible, indicating even a super-reduced state, S_{-2}, also independent of the previous S_0/S_1 ratio. Based on these results corresponding measurements with HA were performed also on isolated PS II complexes from spinach [25], confirming the independence of the S_{-1} and S_{-2} state formation on the previous S_0/S_1 ratio.

With the three-digit backward shift in the O_2 evolution, we observed that this is accompanied by a further new UV-absorption change and a new electrochromic change, respectively, beyond the S_{-1} state. This indicates that in S_{-1} obviously an additional less accessible redox active Mn ion is present in state Mn(III), i.e., S_{-1} (2 Mn(II), Mn(III)); this may be reduced only after stronger treatment with HA, leading to the $S_{-1} \rightarrow S_{-2}$ transition, i.e., the terminal state of the redox-active Mn is S_{-2} (3 Mn(II), see note in Ref. 23). The designation 'redox-active Mn' is used in the following for Mn ions which change reversible their valences between the S_{-2} and S_3 state by reduction with NH_2R and oxidation with light, respectively.

In this work we continue the characterization of the properties of the overreduced S_{-1} and S_{-2} states by examinations of the UV and electrochromic absorption changes and by analysis of the reaction product of the reductant HA by means of mass spectrometry. We outline how the information obtained can be used as a basis for the characterization of the states of redox-active manganese and water in the quaternary S-state cycle from S_0 to S_4.

This work has been presented in part at the Meeting on Electron Transfer Processes in Chemistry and Biology, London (UK), June 1991, and at the Harden Conference, Ashford (UK), September 1991.

Materials and Methods

The oxygen yield per flash and the flash-induced optical absorption changes at 367 nm and 695 nm were measured as described in Ref. 23. Mass spectrometric measurements (MS), especially of $^{15}N_2$ and $^{15}N_2O$ released from oxidized $^{15}NH_2OH$, were performed with Micromass 7070 H/S (VG Instruments) double focusing with E,B configuration. The control of the equipment and analysis of the signals were done with a PDP 11/73 computer (Digital Research) and V.G. 11-250 J software. The MS were digitally scanned from masses of 20 to 60 with an interscan time of 0.5 s up to 8 min. The time-course of the mass signals was recorded and the area indicating the amount of the mass integrated.

O_2-evolving PS II-complexes have been prepared from the cyanobacterium *Synechococcus* sp. according to Refs. 26,27. The PS II stock solutions were diluted

for the measurements with a medium containing 20 mM Mes-Na (pH 7), 0.3 M mannitol, 20 mM $CaCl_2$ and 10 mM $MgCl_2$ (MMCM). DCBQ (600 μM) was used as acceptor to eliminate the binary oscillation of the acceptor side [11]. The preparations were dark-adapted for at least 30 min before measurements. Stock solutions with hydroxylamine and hydrazine were freshly prepared from hydroxylammonium chloride and hydrazinium sulphate (Merck) or $^{15}NH_2OH$ (MSD isotopes) for the MS measurements.

Dark-adapted samples were incubated with indicated concentrations of HA and HH for different times. PD-10 gel filtration columns (Pharmacia) with Sephadex G-25M were used for the removal of the excess reductants as described in Ref. 23.

For MS measurements, the columns were equilibrated with a buffer medium containing 20 mM Hepes-Na (pH 7.5), 0.3 M mannitol, 20 mM $CaCl_2$ and 10 mM $MgCl_2$ (HMCM). The samples were filled in gas-tight 7.5 ml vessels and flushed with He, while being slightly stirred for 4 h. Afterwards, the O_2 yield per flash was measured and either flashes (15 μs duration) were fired and/or HA was injected within ms. After further stirring for 1 h, a sample of the gas phase was injected into the MS inlet. The gas flow into the ion source was regulated with a micro-needle valve (Hoke). Before extracting the gas from the vessels, a constant amount of gaseous $^{18}O_2$ (approx. 2 nmol) was added to each sample. The mass signal 36 was used as an internal standard for correcting the fluctuation of the sensitivity of the equipment. For further details, see text and figure legends. The buffer solution alone evolves already small amounts of $^{15}N_2$ and $^{15}N_2O$ in the presence of $^{15}NH_2OH$; this was taken into account. The

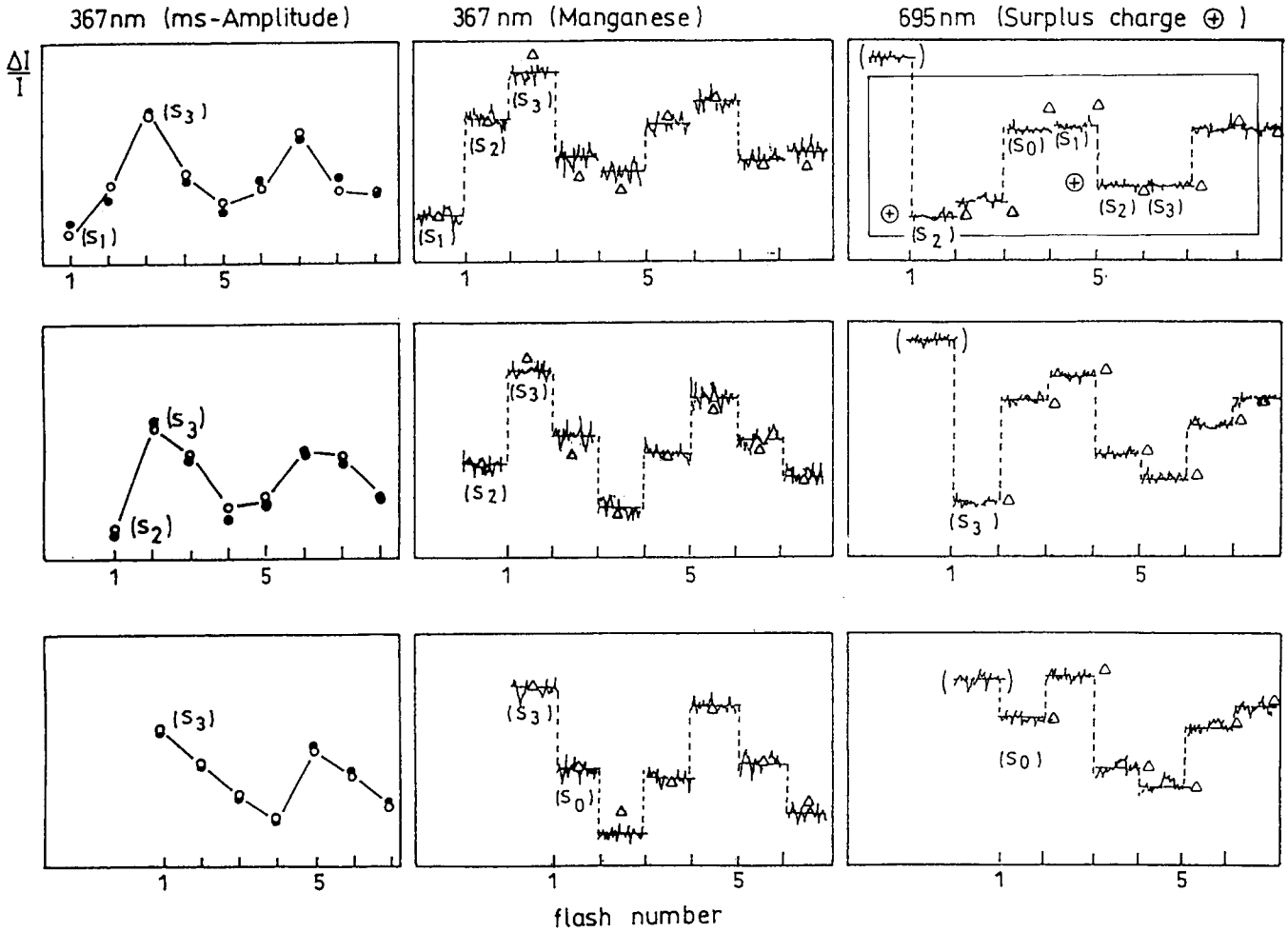

Fig. 1. Oscillation pattern of relative absorption change $\Delta I/I$ as a function of 0, 1, 2 preflashes. Left: Period-four oscillation of the ms amplitude of UV-absorption changes at 367 nm; ○, measured values; ●, calculated values (see text) Center: UV-absorption changes at 367 nm 0.2 s after the flashes. △, calculated values Right: Electrochromic absorption changes at 695 nm 0.2 s after the flashes. △, calculated values. The changes at 695 nm in the first flash are not considered, since they are superposed by an unknown signal, indicated here and in the following by brackets. Top line: without preflash, fitted with 20% S_0, 80% S_1, 5% misses, 8% double hits. Center line: 2 min after one preflash, fitted with 3% S_0, 40% S_1, 54% S_2, 3% S_3, 5% misses, 8% double hits. Bottom line: 2 min after two preflashes, fitted with 10% S_0, 21% S_1, 24% S_2, 45% S_3, 5% misses, 8% double hits. Samples contained in Figs. 1–8 MMCM (pH 7), 5 μM Chl, 600 μM DCBQ as electron acceptor added 1 min before measurements.

MS was calibrated with standard gaseous samples (MSD isotopes). The mass signals, 30 and 46, show a strict linear dependence on the $^{15}N_2$ and $^{15}N_2O$ concentration [28].

Results

Correlation between O_2 evolution, UV and electrochromic absorption changes

Fig. 1 shows the simultaneous measurements of the UV-ms amplitude and the stable UV and electrochromic absorption changes in a train of flashes at different initial S-state distributions. Since in flash light a fraction of the reaction centers does not make a turnover (misses α), while others make a double turnover (double hits β), the S-state transitions become more and more mixed with progressive flash numbers, and the oscillation patterns become progressively damped. O_2 evolution, therefore, takes place not only in the 3rd and 7th, etc., flash but also, to a smaller extent, after each flash with the reverse $S_3 \rightarrow S_0$ transition. The ms amplitude of the UV-absorption change which is coupled with the $S_3 \rightarrow S_0$ transition indicates the extent of O_2 evolution [10,29]. This ms amplitude is shown in Fig. 1, left, for three different initial S-state distributions. Values of the misses and double hits as well as of the initial S-state distribution can be obtained by fitting the measured patterns (open circles in Fig. 1, left) with these parameters (filled circles). We used the obtained parameters and calculated the flash patterns of the quaternary oscillating stable UV-absorption changes with the the three relative $\Delta\epsilon$ values at 367 nm for the $S_0 \rightarrow S_1 \rightarrow S_2 \rightarrow S_3$ transitions [11]. The electrochromic changes at 695 nm can be fitted

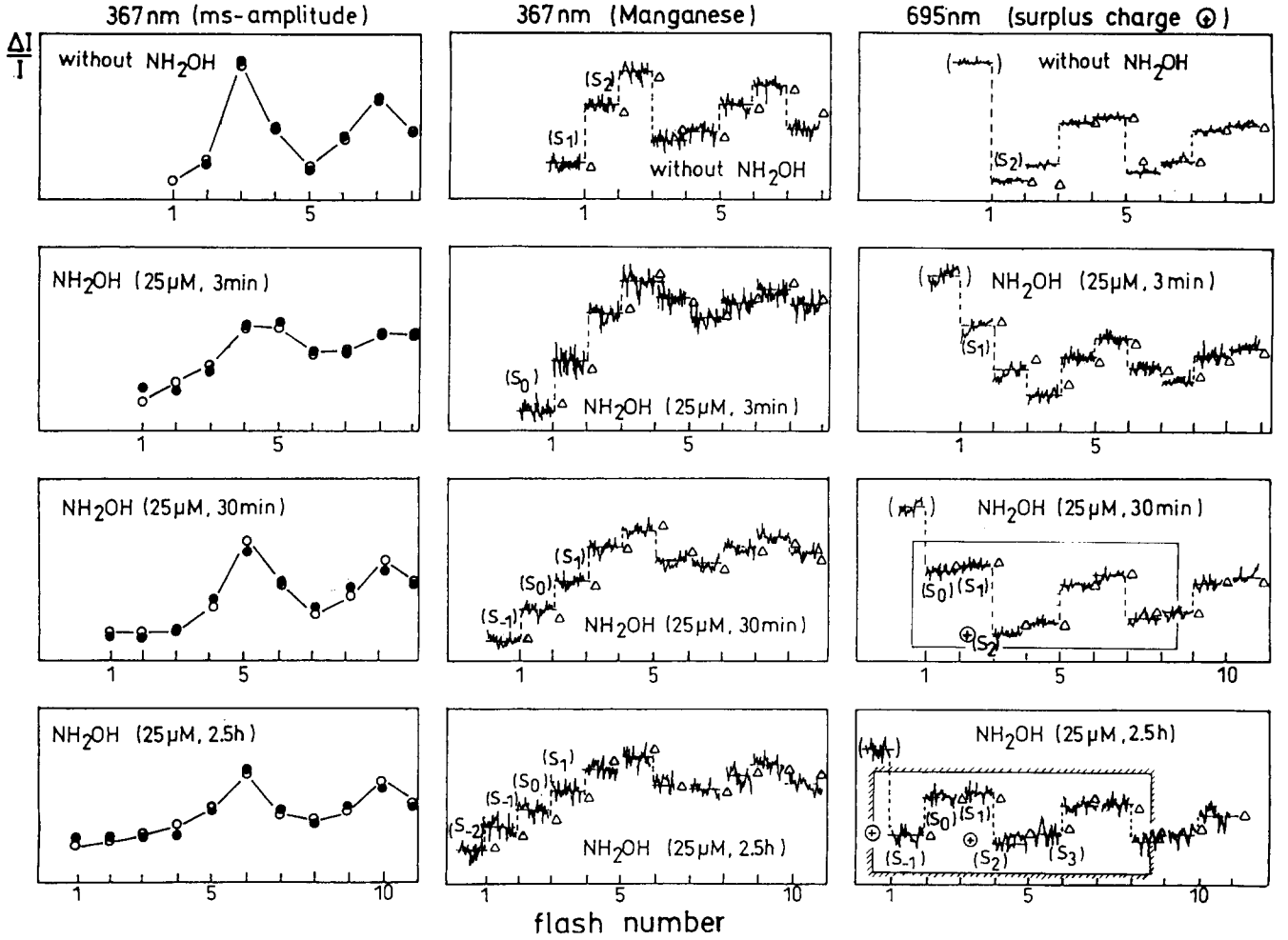

Fig. 2. Oscillation pattern after addition of 25 μM NH_2OH at different incubation times. Left: Period-four oscillation of the ms amplitude of UV-absorption changes at 367 nm; •, measured values; ○, calculated values (see text) Center: UV-absorption changes at 367 nm 0.2 s after the flashes; △, calculated values Right: electrochromic absorption changes at 695 nm 0.2 s after the flashes; △, calculated values. Top line: without NH_2OH treatment, fitted with 33% S_0, 67% S_1, 8% misses, 10% double hits. Second line: incubation with HA for 3 min, fitted with 12% S_{-2}, 53% S_{-1}, 35% S_0, 8% misses, 10% double hits. Third line: incubation with HA for 30 min, fitted with 30% S_{-2}, 65% S_{-1}, 5% S_0, 8% misses, 10% double hits. Bottom line: incubation with HA for 2.5 h, fitted with 100% S_{-2}, 8% misses, 10% double hits. For other details, see Fig. 1.

best for all three different initial S-state distributions if the surplus charges at pH 7 are (0:0:1.1:0.9) in states $S_0:S_1:S_2:S_3$. This is most obvious when the pattern starts with the most unmixed S state (see frame in Fig. 1, right, with 20% S_0, 80% S_1). All measured levels correlate well with the calculated triangles.

The pathway from S_1 via S_0 towards the overreduced S_{-1} and S_{-2} state induced by hydroxylamine in the dark

Fig. 2 shows the patterns of the ms-UV, stable UV, and electrochromic absorption changes with 25 μM HA at different incubation times. In dependence on the incubation time, new levels of absorption changes are created step by step. Already after 3 min incubation time a one-digit shift is observable. After 30 min incubation, a two-digit shift is visible, which is attributed mainly to the overreduced S_{-1} state reported previously [11,18]. After a 5-times longer incubation (2.5 h), a three-digit shift takes place which is denoted as an S_{-2} state. This three-digit shift is also observed in the pattern of directly measured O_2 evolution [24]. The electrochromic change (Fig. 2, right) in all first flashes is superposed by an unknown signal and, therefore, not taken into account (levels in brackets). The misses, double hits and initial S-state distribution were evaluated again by fitting of the UV ms-amplitude pattern (open circle, Fig. 2, left) with these parameters (filled circles). For the fitting of the UV changes in $S_0 \rightarrow S_3$ the same relative $\Delta\epsilon$ values at 367 nm were used as without HA (see Fig. 1). For the $S_{-2} \rightarrow S_{-1}$ and $S_{-1} \rightarrow S_0$ transitions the same $\Delta\epsilon$ value as for $S_0 \rightarrow S_1$ was used. First measurements of the UV-difference spectra of these transitions (Kretschmann, H. and Witt, H.T., data not shown) justified this procedure. The electrochromic changes have been fitted for all four different initial S-state distributions with surplus charges (1:0:0:1.1:0.9) in $S_{-1}:S_0:S_1:S_2:S_3$ (most obvious in the detached frame in Fig. 2, right, with 7% S_0, 86% S_{-1}, 7% S_1, after one flash). The agreement between all measured levels and the calculated triangles is good regardless of the stepwise reverse shift of the S states by HA.

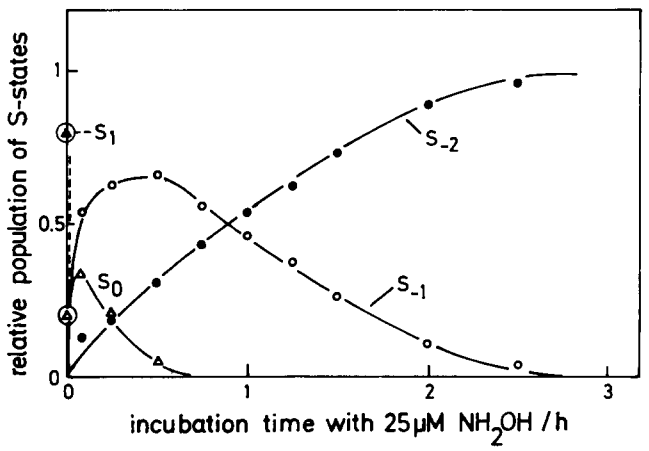

Fig. 3. Course of the relative S-state population as a function of the incubation time with 25 μM NH_2OH. Data obtained from fitting of the ms amplitude of the UV-oscillation patterns at 367 nm with 8% misses, 10% double hits. The initial S_0 and S_1 population of the dark-adapted samples before NH_2OH-treatment is indicated by circles; for other details, see Fig. 1.

Fig. 3 shows the course of the relative S-state population in dark-adapted samples as a function of the HA incubation time. The S-state population was evaluated by the parameters obtained from fitting of the ms amplitude of the UV-absorption changes (O_2 evolution). HA acts as a one-electron donor because of the step-by-step pathway from S_1 via S_0 and S_{-1} to S_{-2}. S_{-1} is an intermediate on the way to the terminal S_{-2} state as observed also from the pattern of O_2 evolution [24]. In contrast to the S_{-1} state the S_{-2} state is, however, much less accessible for a reduction by HA: the S_{-1}-state maximum is reached in approx. 30 min, the S_{-2} state in 2.5 h. The principal course in Fig. 3 is also obtained if, instead of changing the incubation time, the HA concentration is changed (data not shown), or if HH is used instead of HA [28]. With HH a direct conversion of the S_1 to the S_{-1} state occurs, indicating a two-electron donation. The subsequent S_{-2} state is, however, reached through a one-electron donation [28].

Dependence of the overreduced states from the previous S_0/S_1 ratio

In case of a dark reduction of S_1 by a one-electron donor such as HA, the two- or three-digit shift of the S states should be independent of the previous S_0/S_1 ratio. We have shown this with respect to the pattern of O_2 evolution [24] (see Introduction). Fig. 4, left, shows for HA such an independence of the created S_{-1} state with regard to the pattern of UV absorption changes.

In contrast to HA, with HH, a two-digit shift of the O_2 evolution flash pattern depends on the previous S_0/S_1 ratio [21]. In Fig. 4, top, center and right, for the UV and electrochromic absorption changes a two-digit shift towards S_{-1} can be seen at 100% initial S_1 states. However, a three-digit shift towards S_{-2} is observed with the same treatment, when 70% S_0 and 30% S_1 are the initial S states (Fig. 4, bottom, center and right). This has been explained in Refs. 24,25 by a two-electron donation of HH ($S_1 \overset{2e}{\rightarrow} S_{-1}$) and ($S_0 \overset{2e}{\rightarrow} S_{-2}$).

For a comparison of the electrochromic pattern without and after treatment with HA (Fig. 2), the changes treated with HH (Fig. 4) have also been fitted. Agreement between the measured levels and the calculated triangles is obtained if we use for HH the same surplus charges (1:0:0:1.1:0.9) in $S_{-1}:S_0:S_1:S_2:S_3$

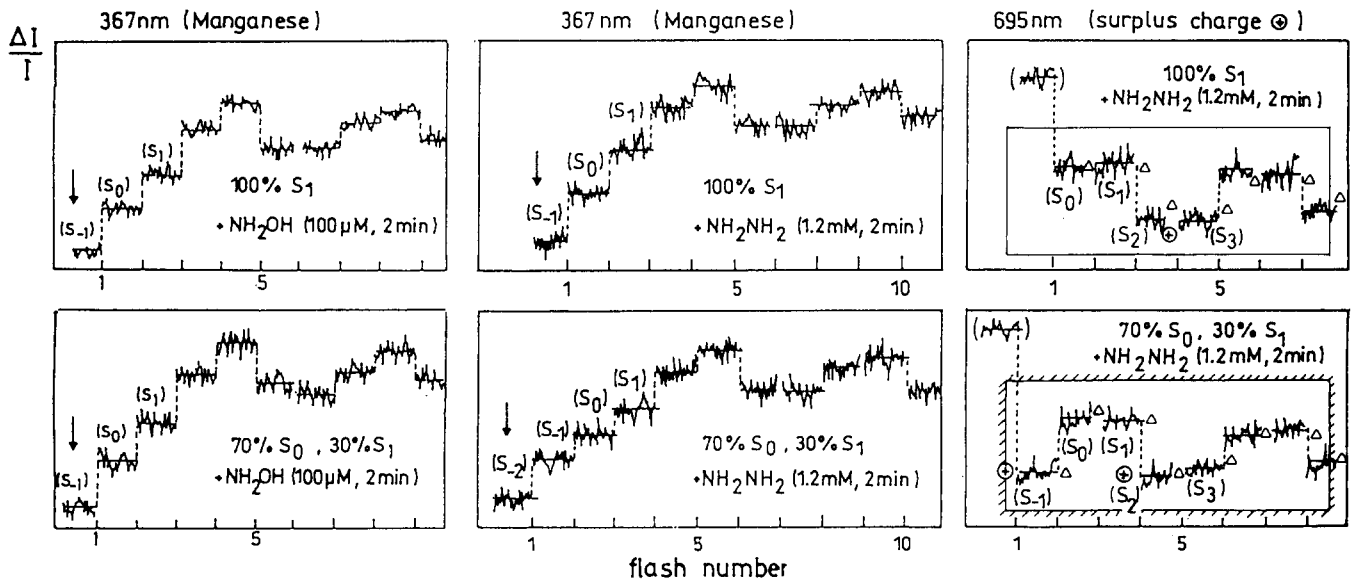

Fig. 4. Oscillation pattern after addition of NH_2R as a function of the previous S_0/S_1 ratio. Top line: 100% S_1 enriched samples. Bottom line: 70% S_0, 30% S_1 enriched samples. Left: UV-absorption changes at 367 nm with 100 μM NH_2OH, after 2 min incubation. Center: UV-absorption changes at 367 nm with 1.2 mM NH_2NH_2, after 2 min incubation. Right: electrochromic absorption changes at 695 nm with 1.2 mM NH_2NH_2 added, after 2 min incubation. Δ, calculated values (see text). 100% S_1 were obtained after one preflash and 20 min dark time. 70% S_0 and 30% S_1 were obtained with three more preflashes on S_1-enriched samples after 10 min darktime. Laser flashes were used; 2% double hits, 10% misses. To avoid interference of S-state reduction with the relaxation of S_0-S_1, higher reductant concentrations were used with shorter incubation times. Other details as in Fig. 1.

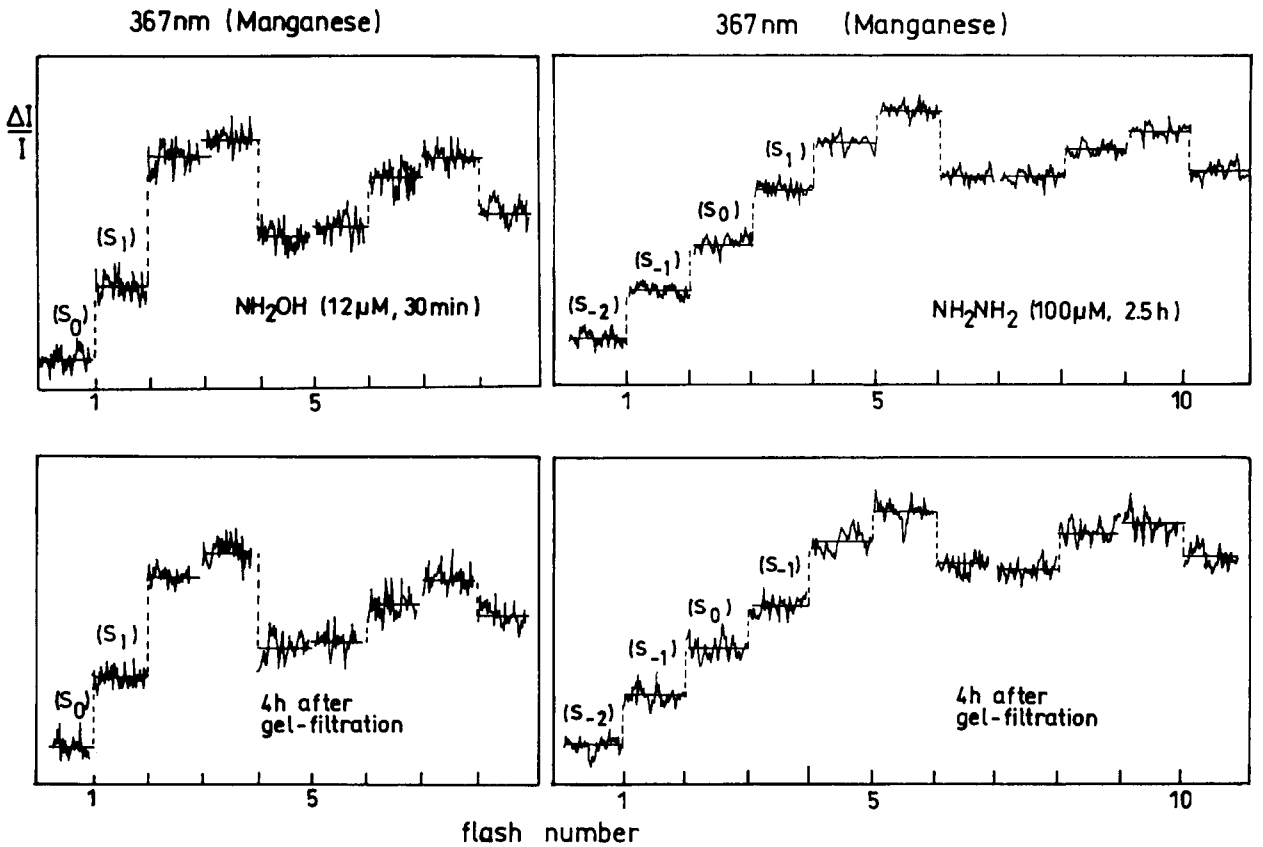

Fig. 5. Stability of the S states reduced by NH_2R. UV-absorption changes at 367 nm. Left, top: incubation with 12 μM NH_2OH for 30 min. Left, bottom: 4 h after removing NH_2OH by gel filtration. The fitting indicates for the first level (top and bottom) 18% S_{-1}, 66% S_0, 16% S_1, 0% S_2, 0% S_3; 8% misses, 8% double hits. Right, top: incubation with 100 μM NH_2NH_2 for 2.5 h. Right, bottom: 4 h after removal of NH_2NH_2 by gel filtration; the fitting indicates for the first level (top and bottom) 100% S_{-2}, 8% misses, 10% double hits. For other details, see Fig. 1.

for the fit as used for HA in Fig. 2. (Obvious in the detached frame in Fig. 4, starting with 10% S_0, 83% S_{-1}, 7% S_{-2}).

Stability of the S_0 and overreduced S_{-1} and S_{-2} states

In a previous report we have shown that the S_{-1} state is maintained for several hours and longer, also after removal of the unreacted HA by very efficient gel filtration [23]. This stability was demonstrated for the two-digit shift of the pattern of O_2 evolution, as well as for the shift of the UV and electrochromic absorption changes indicating a chemical dark reduction of the S_1 state. Fig. 5 supplements this behavior for the stability of the S_0 and S_{-2} states. After removal of HA by gel filtration (Fig. 5, left), the S_0 state, created through the reduction of the S_1 state by HA, remains unchanged for more than 4 h. In Fig. 5, right, the stability is shown for the S_{-2} state created by the reduction with HH. After removal of HH, the S_{-2} state is also stable for more than 4 h.

Treatment of samples in the S_{-2} state with EDTA does not change the O_2-evolving activity (see Fig. 7, filled triangles), indicating a stable Mn configuration in the S_{-2} state.

Regarding the S_{-2} state created by HA, removal of HA does not prevent a very slow oxidation, within 4 h half-time, in the dark towards the S_{-1} state (data not shown). Since HA also reacts with the polypeptides of the surrounding proteins [35], it is possible that under these conditions exogenous electron acceptors (O_2?) can penetrate and can oxidize the S_{-2} state. The principal stability of S_{-2} is documented by the fact that the S_{-2} state, created with the 'soft' reductant HH, is completely stable (Fig. 5, right).

S_{-2} as a reversible terminal state

The S_{-2} state created at incubation times of 2.5 h is a terminal state, because after this time a further step of absorption changes is not observed (Fig. 3); i.e., a reversible state beyond S_{-2} does not exist. To exclude slow kinetics as a reason for an apparent termination, we introduced a second new charge of HA and HH, respectively, after formation of the S_{-2} state. Before this was done, the unreacted reductants of the first charge were removed by gel filtration. After an additional 3–4 h incubation time, no further shifting is visible (see Fig. 6), but a further deactivation of the samples can be observed (see Fig. 7). The existence of a stable terminal S_{-2} state is understandable if the redox-active Mn ions are fully reduced to state Mn(II). S_{-2} does not exhibit a six-line EPR signal of MnII (x-band).

Deactivation of the S_{-2} state and Mn depletion

In the presence of HA or HH the samples become increasingly deactivated with increasing incubation time

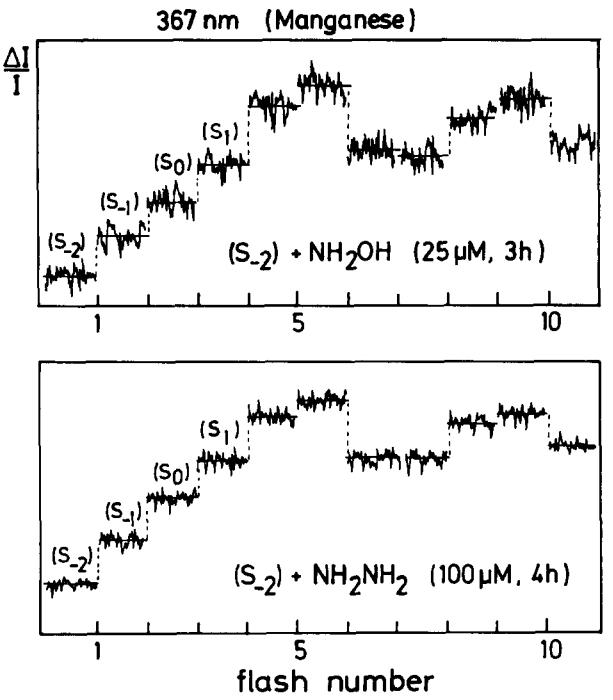

Fig. 6. S_{-2} as a terminal overreduced state. UV-absorption changes at 367 nm. Top: 3 h after addition of 25 μM NH_2OH to samples in state S_{-2} (prepared with NH_2NH_2 and subsequent removal by gel filtration). Bottom: 4 h after addition of 100 μM NH_2NH_2 to samples in state S_{-2} (see Top). For other details, see text and Fig. 1.

(Fig. 7). At the point of the incubation time (2.5 h), where the sample is reduced completely by HH via S_0 and S_{-1} to pure S_{-2} states (100%), 70% of the amount

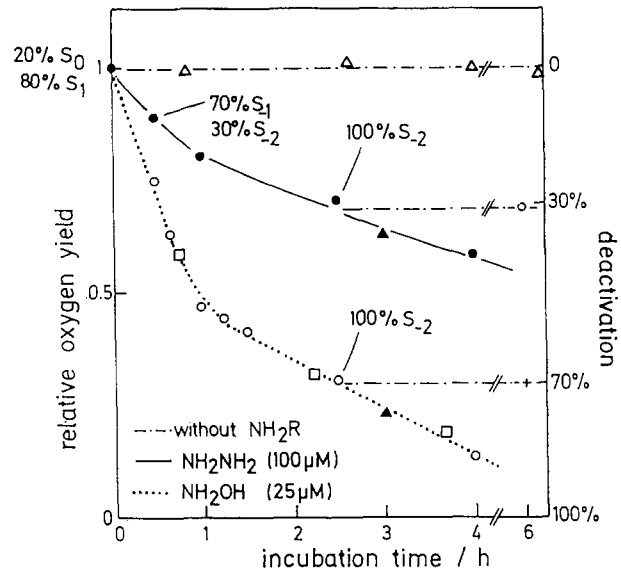

Fig. 7. Relative oxygen yield as a function of the incubation time with 100 μM NH_2NH_2 and 25 μM NH_2OH, respectively. The indicated S-state distribution of the active complexes was obtained from UV measurements. △, without NH_2R; ●, incubation with 100 μM NH_2NH_2; ○, incubation with 25 μM NH_2OH; ▲, S_{-2} samples incubated with 60 mM EDTA for 2 h; □, buffer medium with 2.5 mM $CaCl_2$ instead of 20 mM $CaCl_2$, 2 mM FeCy plus 200 M PPBQ as electron acceptor. For other details, see text and Fig. 1.

of OEC that were previously present (20% S_0, 80% S_1) is in S_{-2} and 30% is deactivated. Obviously, during the incubation time in the case of HH, 30% of the created S_{-2} states were subsequently converted into non-functional complexes. Using HA, 30% of the original amount of OEC is in S_{-2} and 70% is deactivated. This indicates a much higher degree of aggressiveness of HA than HH on the protein environment (see Stability of the S_0 and overreduced S_{-1} and S_{-2} states). When the incubation time was extended above 2.5 h, all S_{-2} states were finally converted to non-functional complexes. The deactivation occurs with the permanent depletion of the Mn ions from the S_{-2} state into the solution, because samples deactivated by HA and HH, respectively, have in the end lost all Mn ions [51]. After all states are converted after 2.5 h to S_{-2} states and in part into deactivated complexes, the S_{-2} state is stable and the O_2 yield remains unchanged for hours after removal of the unreacted NH_2R by gel filtration (dotted lines in Fig. 7).

Examination of the products of the reductant HA by mass spectrometry

It would be worthwhile to examine the properties of the overreduced S states additionally by chemical analysis of the behavior of the immediate reactant of the S state, i.e., of the products of the reductant HA.

N_2 evolution from HA in O_2-evolving samples was first observed by Radmer and Ollinger [20], but with amounts much too low to support the dark reduction of S states by HA (see Discussion in Ref. 11). N_2 evolution after flash-light excitation of samples deactivated (a) by incubation with 1 mM HA was reported in Ref. 30, and (b) by treatment with Tris was reported in Ref. 31. In the latter work, normal samples show the same N_2 evolution when treated with HH as with Tris, from which it was concluded that N_2 evolution is not correlated with the S-state change. In Ref. 32, with material from cyanobacteria, Tris treatment, however, strongly effects the N_2 evolution, and it was stated that HH oxidation deactivates the S-state system to a state reduced beyond S_0.

In the following, we will give mass spectrometric evidence that HA is oxidized in the dark simultaneously with the S-state reduction. The oxidation of $^{15}HA(^{15}NH_2OH)$ was recognized by a $^{15}N_2$, as well as by a $^{15}N_2O$ evolution. N_2 is very probably formed after an oxidation of 2 HA through the S states:

$$2NH_2OH \xrightarrow{-2e} 2NH_2O + 2H^+ \rightarrow N_2 + 2H_2O + 2H^+$$

as discussed in Ref. 30 on the basis of HA reactions with transition metals in vitro. The N_2O evolution is practically only observed when the Mn ions are released into the solution. N_2O may thereby result from a four-electron oxidation of 2 HA [33]:

$$2NH_2OH \xrightarrow{-2e} 2NH_2O + 2H^+ \xrightarrow{-2e} 2NHO + 4H^+$$

$$\rightarrow 1N_2O + H_2O + 4H^+$$

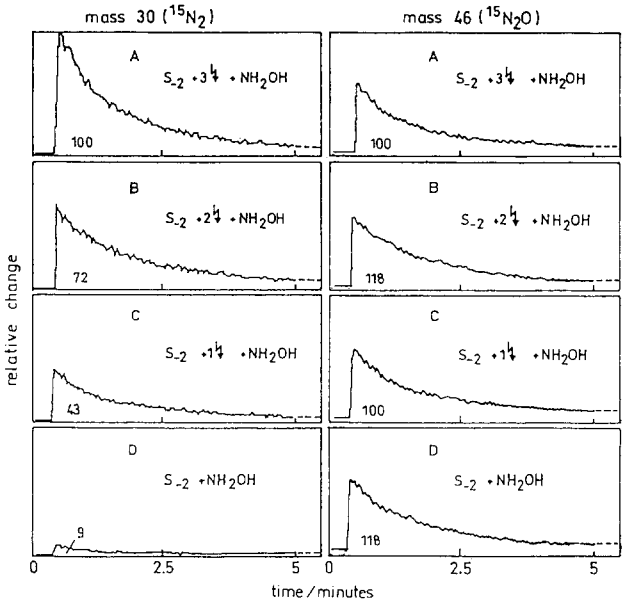

Fig. 8. Left: Relative $^{15}N_2$ evolution, measured by mass spectrometric analysis at mass 30 of four samples, A–D, treated with 100 μM $^{15}NH_2OH$ for 1 h. A 'clean' sample, with active complexes only in state S_{-2}, was used as a basis (S_{-2} was prepared from S_1 by incubation with 100 μM NH_2NH_2 for 2.5 h and subsequent removal of NH_2NH_2 by gel filtration). (A) Treated after three flashes; (B) treated after two flashes; (C) treated after one flash; (D) treated directly S_{-2}. For details, see text. Right: Relative $^{15}N_2O$ evolution measured at mass 46 under the same conditions as described above.

The experimental accuracy of the $^{15}N_2$, as well as of the following $^{15}N_2O$ measurements is $\pm 25\%$.

In a thorough analysis of N_2 evolution in preceding experiments, we observed that the smaller the O_2-evolving capacity of the preparations the larger the N_2 evolution from NH_2OH, which is not coupled with the reduction of the S states. This 'background' N_2^* created by unknown side reactions can be eliminated as follows. Samples are converted to pure S_{-2} states (100%) with HH (100 μM, 2.5 h) (Fig. 7). Thereby, N_2^* is evolved as well as the N_2 presumed to be coupled with the $S_1 \rightarrow S_{-2}$ transition. Subsequently, the sample in the S_{-2} state is stabilized by removal of the unreacted HH and elimination of contaminations by gel filtration. This 'clean', stable S_{-2} sample is no longer active in N_2 evolution after renewed incubation with HA (see Fig. 8, left, bottom and Table I, right). 'Clean' S_{-1}, S_0 and S_1 states are created by excitation of this S_{-2} sample with 1, 2 and 3 single-turnover flashes. Because of misses (5–10%) and double hits (approx. 5%) the flash-induced states S_{-1}, S_0 and S_1 are not formed completely. Therefore, only (80–90%) S_{-1},

TABLE I

$\frac{1}{2}$ $^{15}N_2$ and $\frac{1}{4}$ $^{15}N_2O$ evolution per OEC from S_{-2} samples treated with $^{15}NH_2OH$ (100 μM 1 h) after the indicated flashes were fired

* Relative; ** absolute calibration. For details, see text.

	$S_{-2}+3$ ↯	$S_{-2}+2$ ↯	$S_{-2}+1$ ↯	S_{-2}
Transition	(S_1)-Sol	(S_0)-Sol	(S_{-1})-Sol	(S_{-2})-Sol
$\frac{1}{2}$ $^{15}N_2$ *	3.0	2.1	1.1	0
$\frac{1}{2}$ $^{15}N_2$ **	3.1	2.2	1.2	0.2
$\frac{1}{4}$ $^{15}N_2O$ **	–	–	–	3.7

(70–80%) S_0 and – considering the fast S_2 relaxation in the presence of Tyr-160 [28] (see Discussion) – (75–85%) S_1 states will be present. The brackets in Table I are included to point out this restriction.

(a) Each of the 'clean' S_{-2}, (S_{-1}), (S_0) and (S_1) states was treated in the dark with HA (100 μM, 1 h), which led to a decrease of the O_2 evolution down to 4% (data not shown). It was shown that with this deactivation nearly all Mn ions were released and swept out into the solution [51]. In each of these treatments the oxidation of HA was followed by mass spectrometric analysis of the evolved $^{15}N_2$ (mass 30) and $^{15}N_2O$ (mass 46). With respect to the N_2 evolution, the result is shown in Fig. 8A–D, left. The $^{15}N_2$ amount observed with the Mn release from S_{-2} into the solution Sol (D) is approx. 5-times smaller than in C. This value is far too low to be due to a one-electron oxidation of HA. The small signal in D is subtracted as background from A, B, C and D. The corrected values for these transitions are then 91, 63, 34, and 0. The relative difference of $^{15}N_2$ between A-B, B-C and C-D corresponds to the $^{15}N_2$ evolution per flash and is, on the average, 30 units. This value must correspond to a one-electron oxidation of one HA molecule per OEC and S-state transition. This indicates that a approx. 3,2,1-electron reduction per OEC, predominantly of states S_1, S_0 and S_{-1}, has taken place and a approx. 3,2,1 evolution of $\frac{1}{2}$-$^{15}N_2$, respectively (see Table I). Negligible N_2 evolution is observed with the irreversible deactivation of S_{-2} and Mn depletion.

(b) The values in Table I, asterisk, were obtained by using the difference of N_2 evolution between A-B, B-C, and C-D, respectively, as standard for the one-electron oxidation of one HA per OEC. In the following, this was also evaluated by the absolute measurement of $^{15}N_2$ and OEC: the released $^{15}N_2$ was directly calibrated with a standard $^{15}N_2$ gas probe and the OEC estimated by the absolute O_2 measurement per flash. The result is shown in Table I, second line, and agrees with the first line.

(a′) In contrast to this $^{15}N_2$ evolution, in the above described S_n-S_{n-1} transition steps $^{15}N_2O$ evolution is practically not observed. This is shown by the approximately constant $^{15}N_2O$ evolution in Fig. 8A–D, right. From D, however, it is evident that this evolution is created in the $S_{-2} \rightarrow$ solution transition in which the Mn depletion takes place and where no further shift of the S states is observed (see Deactivation of the S_{-2} state and Mn depletion).

(b′) Also, with N_2O, absolute measurements were carried out. For the $S_{-2} \rightarrow$ solution transfer, a value of $3.7\frac{1}{4}$ $^{15}N_2O$ per OEC was found (Table I). This corresponds to an approx. 3–4-electron difference between the S_{-2} state and the solution. We also observed the same evolution of $^{15}N_2$ and $^{15}N_2O$ when HA (25 μM, 2.5 h) instead of HH was used for the formation of 'clean' S_{-2} preparations.

The conclusion is that there is a three-electron difference on the reversible pathway between the redox-active Mn ions in the S_1 and S_{-2} states. In each of the reversible individual transitions, $S_1 \rightarrow S_0$, $S_0 \rightarrow S_{-1}$, $S_{-1} \rightarrow S_{-2}$, a one-electron reduction is indicated by approx. 1/2-$^{15}N_2$ evolution and oxidation of 1 HA per OEC. This was measured also for the transitions $S_3 \rightarrow S_2$ and $S_2 \rightarrow S_1$ starting from S_1 on with two and one flashes, respectively (data not shown). On the irreversible path of the S_{-2} state deactivation and Mn release into the solution no $^{15}N_2$ evolution takes place but an approx. 1 ·$^{15}N_2O$. This indicates that deactivation and Mn depletion are coupled with a approx. four-electron reduction of the system by 2 HA.

Discussion

Correlation between ms amplitudes, UV- and electrochromic changes in the entire S-state range from S_{-2} to S_3

(i) The period-four oscillation of ms amplitudes, and of the stable UV and electrochromic absorption changes in the $S_0 \rightarrow S_3$ forward transition can be described by one and the same set of parameters regardless of the very different initial S-state distribution (Fig. 1). Therefore, all three signals reflect properties of one and the same process: the cycling of the S states. (ii) This three-fold correlation is also visible in the synchronized backwards shift from S_1 to the S_{-2} state after different incubation times with HA (Fig. 2). (iii) The conversion of the initial S_1 state into the S_{-2} state takes place like a serial reaction sequence going through the intermediates S_0 and S_{-1} (Fig. 3). (iv) As the $S_1 \rightarrow S_3$ pattern starting from S_1 is the same as the $S_1 \rightarrow S_3$ one, when the sequence starts with the S_{-2} state after HA treatment, indicates that an intermediate exposure to HA does not change the quality of the subsequent native $S_0 \rightarrow S_4$ cycling. (i)–(iv) indicate that probably the same reactants – Mn ions and water – change their states backward and forward between the S_{-2} and S_3 state.

The pathway to the S_{-2} state – S_0/S_1 dependence

The step-by-step reduction in Figs. 2 and 3 is evidence for the one-electron donor capacity of HA. A paramagnetic product of HA was, however, not observed [22,34]. This may be due to a fast recombination of two nitrooxide radicals producing N_2 as final product. The latter has been observed (see Results). Because of the absence of the radicals, it was suggested in Ref. 22 that HA acts as a two-electron donor, creating an S_{-1} and S_{-3} state without formation of the here discussed S_{-2} state. This conclusion is, however, not confirmed by our results.

The independence of the creation of the S_{-1} and S_{-2} state from the previous S_0/S_1 ratio, shown for the O_2-evolution pattern in Ref. 24 and observed optically in Fig. 4, left, indicates again a dark reduction of the S_1 state by means of HA. That HH also reduces the S states in the dark although in this case the S_{-1} and S_{-2} population depends on the previous S_0/S_1 ratio [21], which is shown also for the UV- and electrochromic absorption changes in Fig. 4, center and right, is explained on the basis of a two-electron donation from HH. HH reduces in one step S_1 to S_{-1} and S_0 to S_{-2}. Therefore, these products reflect the previous S_1/S_0 ratio in contrast to the reduction with HA [24,25].

Stability of the reduced S_0, S_{-1} and S_{-2} states and Tyr-160 reduction

The states created from S_1 after sufficient incubation times with HA and HH, respectively, i.e., S_0 (Fig. 5), S_{-1} [22] and S_{-2} (Fig. 5) are stable after subsequent removal of the unreacted reductant by gel filtration. This further supports the fact that S_1 is reduced in the dark.

Under normal conditions, without HA, the S_0 state is unstable and is transformed in the dark to S_1 within approx. 20 min [38]. The oxidized Tyr^+-160 of the D2 protein is supposed to be the electron acceptor [36]. Obviously, HA has not only reduced S_1 to S_0 in the dark, but also simultaneously Tyr^+-160, thereby preventing the $S_0 \rightarrow S_1$ transfer. We have observed this with the analysis of the EPR signal II_{slow} of Tyr-160 (data not shown). This reduction of Tyr^+-160 becomes also visible by the observation that in the presence of HA the fast component of the S_2 relaxation (approx. 1.5 s) [38] – attributed to Tyr-160 oxidation [5] – is increased in HA-treated samples from 20% to 60% [28].

The Tyr^+-160 reduction by HA was shown for the preparation for the cyanobacteria material used here. In higher plants, however, a reduction of Tyr^+-160 by low HA concentrations has not been observed. This takes place only after Mn has been depeleted from the samples [22,34].

The consequence of our observation is that besides the oxidation of HA by means of the reduction of the S states, one HA must be used for the reduction of Tyr^+-160, which should lead to $\frac{1}{2}$ $^{15}N2$ evolution. However, the essential feature of the experiments in Fig. 8 and Table I is to have used samples A,B,C,D prepared from complexes previously converted by HH to pure S_{-2} states (100%). Under these conditions, Tyr-160 has also been reduced (see Stability of the S_0 and overreduced S_{-1} and S_{-2} states). The HA oxidation and N_2 evolution, respectively, in reaction with the subsequently flash-induced (S_1), (S_0), (S_{-1}) states (see Examination of the products of the reductant HA by mass spectrometry) are, therefore, indicating only the reduction of the S states.

It should be pointed out that in all flash-induced oscillation patterns, when HA or HH is present, an additional relaxation of the S_2- and S_3-states by the reductants (HA,HH) or by Tyr-160 does not take place, because the flash frequency (0.1–0.2 s) used is much faster than the reduction times.

S_{-2}: a reversible terminal state

The S_{-2} state is the most reduced reversible state and, thus, the terminal state, because neither longer incubation times (4 h) nor additional support with fresh reductants leads to a change of the pattern to an S_{-3} state (Fig. 6). The existence of S_{-2} as the final reduced state makes it probable that in S_{-2} the redox-active Mn ions are present in the lowest level, i.e., as Mn(II) ions exclusively.

Recently, the formation of a so-called stable pool of Mn(II) was reported [39,40]. This pool was created with HA (or hydroquinone) from membranes of higher plants depleted of extrinsic proteins but stabilized by means of higher concentrations of Ca^{2+}. It should represent a temporarily stable form similar to the labile S_{-3} state postulated in Ref. 22, which should precede inhibition of O_2 evolution and Mn^{2+} release into the solution. This reversible state is probably not comparable to the terminal, reversible stable S_{-2} state discussed in this work: The state in Ref. 39 is sensitive to EDTA exposure which causes a concurrent loss of Mn. The S_{-2} state described here is insensitive to EDTA treatment (see Stability of the S_0 and overreduced S_{-1} and S_{-2} states). Subsequently, we have also checked protection against deactivation by Ca^{2+} as described in Ref. 39. This was not observed in our system, either (open squares in Fig. 7).

Correlation between the S-state reduction and N_2 evolution from HA: three reducible and photooxidable Mn ions and their possible valence states

The three-digit reverse shift of the oscillation pattern of (i) O_2 evolution [24]; (ii) the UV-absorption changes of Mn, and (iii) the electrochromic change of charges are quantitatively coupled at each of the three

steps of the shift $S_1 \rightarrow S_0 \rightarrow S_{-1} \rightarrow S_{-2}$ with approx. $\frac{1}{2} \cdot {}^{15}N_2$ evolution and oxidation of one HA molecule per OEC, respectively (Fig. 8). This indicates a one-electron reduction in each of these steps and a three-electron difference between S_1 and S_{-2}. Since also the S_2 and S_3 states and Mn ions, respectively, are reducible by HA, coupled with corresponding amounts of N_2 evolution (see Results), each backwards step from S_3 on is coupled with $\frac{1}{2} \cdot {}^{15}N_2$ evolution. Since no N_2 evolution takes place in the Mn depletion from S_{-2} into the solution (Table I), this means that all redox-active Mn ions should stay in S_{-2} as Mn(II). The valence states of the Mn ions up to S_3 can be evaluated as follows. The conclusion (a) that the S_{-2} state is the final reduced state with the redox-active ions at the Mn(II) level and (b) the result that there is a three-electron-difference between the redox-active Mn ions in S_1 and S_{-2} can be explained if in the S_1 state two, three or four redox active Mn ions are present with valences of (III, IV), (III, III, III), (II, III, IV), (II, III, III, III) or (II, II, III, IV). S_1(III, IV) is ruled out because it cannot be oxidized up to S_3 if in vivo Mn(IV) is the highest oxidation state, as generally supposed. The S_1 states with Mn(II), considered to be oxidized in the $S_1 \rightarrow S_2$ or $S_2 \rightarrow S_3$ transitions, are excluded according to the result that no Mn(II) is detected in S_1 [48]. With this 'selection' of S_1(3 Mn(III)), consequently, the photo-oxidizable parts of the S states should be S_{-2}(3 Mn(II)), S_{-1}(2 Mn(II), Mn(III)), S_0(Mn(II), 2 Mn(III)), S_1(3 Mn(III)), S_2(2 Mn(III), Mn(IV)) and S_3(Mn(III), 2 Mn(IV)) (see Fig. 9, top).

The S-state sequence indicates that the $S_0 \rightarrow S_1$ transition (Mn(II) $\rightarrow$ Mn(III)) is different from equal changes (Mn(III) $\rightarrow$ Mn(IV)) in $S_1 \rightarrow S_2$ and $S_2 \rightarrow S_3$. This result is in line with the UV-difference spectra of these transitions: In the original work on UV absorption changes of Mn equal changes were measured for all $S_n \rightarrow S_{n+1}$ transitions [10]. We have, however, shown in Ref. 11 that the UV-difference spectrum of the $S_0 \rightarrow S_1$ transition is different from the spectrum of the $S_1 \rightarrow S_2$ and $S_2 \rightarrow S_3$ transitions; the latter two are similar. At 355 nm the $\Delta\epsilon$ ratio is about $\Delta\epsilon_{01} : \Delta\epsilon_{12} : \Delta\epsilon_{23}$ approx. 0.5 : 1 : 1. The smaller changes of $S_0 \rightarrow S_1$ were also observed in Ref. 41 (see also the more recent results in Refs. 42,43; that the spectrum for $S_0 \rightarrow S_1$ is even zero as claimed in Ref. 43 has not been confirmed). It should be mentioned that in the case of equal valence changes in $S_1 \rightarrow S_2$ and $S_2 \rightarrow S_3$ one does not expect completely equal difference spectra, because very probably in the S_1–S_3 states different Mn ligands (e.g., water derivatives, see Fig. 9) and different conformations, respectively, are present which would allow only a similarity in the difference spectra). Conclusions from ESR and XAS measurements support that valence changes in $S_1 \rightarrow S_2$ and $S_2 \rightarrow S_3$ transitions are equal (Mn(III) $\rightarrow$ Mn(IV)) and different

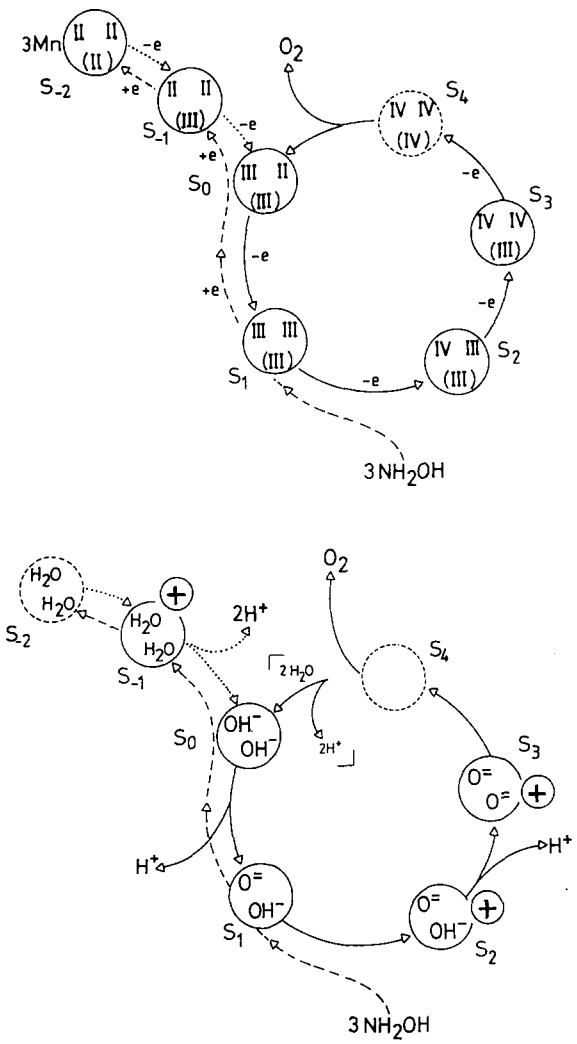

Fig. 9. Top: Possible valence states of the redox-active Mn ions in the $S_0 \rightarrow S_3$ states and in the states S_{-1} and S_{-2}, overreduced by HA and HH, respectively. Bottom: Possible states of water and surplus charges, ⊕, at pH 7 in the $S_0 \rightarrow S_3$ states and in the states S_{-1} and S_{-2}, overreduced by HA and HH, respectively. For details, see text.

from the $S_0 \rightarrow S_1$ one. This is outlined at the end of this section.

The assignment of the Mn valences in Fig. 9, top, is in agreement with the shift as well as with the energy of the X-ray K-edge of Mn and conclusions from NMR proton relaxations:

With regard to the $S_0 \rightarrow S_1$ and $S_1 \rightarrow S_2$ transitions, both are accompanied by a K-edge shift to higher energy, indicating two oxidation steps of Mn [44]. Recently, also for the $S_2 \rightarrow S_3$ transition a further shift to higher energy has been measured at room temperature, which was interpreted in the simplest way as one more oxidation of an Mn(III) ion upon this transition [45]. However, the K-edge shift in $S_2 \rightarrow S_3$ was not observed in Ref. 46, possibly because the latter work was carried out at cryogenic temperatures at which the S-state transition may be different. We had pointed out

already in Ref. 23 that redox-active amino acids could be in a redox equilibrium with Mn and that at low temperature there can be a noticeable shift in the S states towards the acids. Therefore, Mn reduction would not be visible in these states at low temperature (for details, see Ref. 23).

After addition of NH_2OH at a low concentration, recent XAS measurements indicated a reversible K-edge shift of Mn from S_1 to lower energy [47]. This is in line with our observation of Mn over-reduction towards the S_{-1} and S_{-2} states, respectively. These results also exclude the possibility that NH_2R reduces unknown substances [25]. The absence of a K-edge shift to lower energy in the presence of NH_2OH as measured in Ref. 46 has to be clarified.

In respect to the energy of the K edge, it was followed that only Mn(III) and/or Mn(IV) are present in the S_1 and S_2 state [48]. Mn(II) was concluded to be located in S_0 [46]. Based on NMR measurements of proton relaxation, an Mn(III)-Mn(IV) change was considered for the $S_2 \rightarrow S_3$ transition [49], in contrast to previous conclusions [50].

Together with the result on the K-edge shift (see above), it follows from the latter paragraph that the $S_1 \rightarrow S_2$ and $S_2 \rightarrow S_3$ transitions should both be due to Mn(III) $\rightarrow$ Mn(IV) changes and the $S_0 \rightarrow S_1$ transition due to an Mn(II) $\rightarrow$ Mn(III) oxidation (see also Ref. 60).

The $S_3 \rightarrow S_4$ transition remains 'invisible' with regard to UV-absorption changes and to analysis by other methods because of the immediate re-reduction of all redox-active Mn ions in the $S_4 \rightarrow S_0$ transition. But, possibly the third redox-active Mn(III) ion in S_3 (in brackets) is oxidized to Mn(IV) in S_4 (see Fig. 9, top). This suggestion is indicated by a dotted circle.

The redoxactive and the total amount of manganeses in the OEC

The Mn-valence states in the S-state cycle from S_{-2} up to S_3 refer only to Mn ions which change their valences in the cycling of the water splitting complex. The conclusion is that up to the S_3 state three redox-active Mn ions – not two and not four – are consistent with the two statements (a) and (b) (see beginning of the preceding section). The consequence of the above outlined argumentation is that further Mn ions present in the Mn complex must be redox-inactive.

It is commonly accepted that four Mn ions per OEC do exist. In this case, the fourth Mn ion must be redox inactive over the entire S-state range S_{-2}–S_3 and must stay in state Mn(III) or Mn(IV), since Mn(II) is not present in S_1 [48]. In the case of 6 Mn per OEC [51], three Mn must stay redox-inactive in state Mn(III) or Mn(IV). The N_2O evolution from HA, coupled with the irreversible Mn release shown in Fig. 8 and Table I, may be in connection with this inactive Mn fraction. Instead of N_2 a approx. 1 $\cdot {}^{15}N_2O$ evolution per OEC is observed after ^{15}HA treatment of the S_{-2} state, indicating that the Mn release is coupled with a approx. 3–4-electron reduction of the complex by approx. 2 HA. The N_2O evolution may be involved in the reduction of non-redox-active Mn ions, still being in the S_{-2} state in higher oxidation states than Mn(II) (see above).

The release of the Mn ions into the solution may, however, also be due to the specific reduction of unknown 'anchors' of the Mn ions by HA with N_2O evolution as oxidation product. This may be the opening of the ligands between the Mn ions and the surrounding proteins. Furthermore, the reaction with residues accessible in the depleted complex may be considered. Although a decision regarding the mechanism of the N_2O evolution is not possible as yet, further analysis of this reaction may give information on the structure of the Mn cluster and how it is stabilized within the frame of the surrounding proteins.

The surplus charges and deprotonations

The electrochromic pattern identified through the characteristic chlorophyll difference spectrum [14] indicates at pH 7 the creation of positive surplus charges in the S_2 and S_3 states. This result was independently obtained by observation of an up to 10-times slower electron transfer time from the S_2 and S_3 states, respective to the oxidized Chl a_{II}^+ (P_{680}^+) [15]. The result in Refs. 14,15 of net charges (0:0:1:1) in $S_0:S_1:S_2:S_3$ is explained if with the $S_0 \rightarrow S_1 \rightarrow S_2 \rightarrow S_3$ oxidations an H^+ release of (−1:0:−1) takes place (see Fig. 9). This result is identical with earlier results obtained with pH indicators in Ref. 52. In this work, the electrochromic patterns have been measured at very different conditions, whereby at pH 7 a small non-integer stoichiometry becomes visible. The changes at three different initial S-state distributions (Fig. 1), as well as the four changes obtained after different treatment with HA and HH, respectively (Figs. 2 and 4), can be computed commonly with (0:0 1,1:0,9) net charges in $S_0:S_1:S_2:S_3$. This non-integer ratio at pH 7 would correspond to an H^+ release of (−1:0,1:−1,2:−1,9) with the $S_0 \rightarrow S_1 \rightarrow S_2 \rightarrow S_3 \rightarrow S_0$ transition. The 1.9 protons released in $S_3 \rightarrow S_0$ is simply the complement to the 4 H^+ released in one turnover.

Considering now also the electrochromic pattern in the range of the over-reduced S states (Figs. 2 and 4, right) we observe that the electrochromic change in the first flash is overlapped by an unknown signal. However, the genuine change between S_{-1} and S_0 is independent of such an artefact and always available when the $S_{-1} \rightarrow S_0$ transition takes place in the 2nd flash; i.e., after a three-digit shift has been induced by NH_2R (see hatched frame in Figs. 2 and 4, right, bottom). The jump from S_{-1} to S_0 in the second flash indicates that a net charge in S_{-1} disappears with the S_0 formation

and is explained by the accompanying release of two protons. The extended pattern starting with S_{-1} can be fitted commonly at pH 7 with (1:0:0:1.1:0.9) net charges in $S_{-1}:S_0:S_1:S_2:S_3$. This would correspond to a release of H^+ (−2: −1:0.1: −1.2) with the $S_{-1} \rightarrow S_0 \rightarrow S_1 \rightarrow S_2 \rightarrow S_3$ transition. The release of 2 H^+ with the $S_{-1} \rightarrow S_0$ transition was concluded also from pH indicator measurements [19].

(A) A non-integer stoichiometry of H^+ release in the $S_0 \rightarrow S_3$ range was first observed with pH indicators especially above and below pH 7 [53]. The H^+ stoichiometry measured in Ref. 53 for the $S_0 \rightarrow S_1 \rightarrow S_2 \rightarrow S_3$ transition at pH 7 is (−1,1: −0,25: −1,0). This result is not very different from our ratio (−1,0:0,1: −1,2) at pH 7. The non-integer phenomenon was explained by pK shifts of neighbouring amino-acid residues and pH-dependent transient H^+ releases, respectively. The shifts should be induced by the electric field of the positive charge created at the Mn complex with the $S_n \rightarrow S_{n+1}$ oxidation.

(B) It is, however, possible to explain non-integer H^+ stoichiometries also by making use of pH-dependent water states. With a pH change from 8 to 5 the state of water, as well as the charge of the S states, may change in each of the S_0-S_3 states from, e.g., $S_n(2OH^-)$ to S_n^{1+} (H_2O, OH^-) and further to S_n^{2+} ($2H_2O$). In Ref. 63 this shift was made responsible for the pH-dependent electron transfer times between the S states and Chl a_{II}^+ ($P680^+$). pK shifts induced by the electric field of the subsequent $S_n \rightarrow S_{n+1}$ oxidation would release protons from these water states. The simultaneous presence of the two neighboring S states (at appropriate pH values) would result in a pH-dependent non-integer stoichiometry, e.g., $S_n(2OH^-) - \frac{1}{2}\ H^+ \rightarrow \frac{1}{2}\ S_{n+1}^{1+}\ (2OH^-) + \frac{1}{2}\ S_{n+1}\ (OH^-, O^{2-})$. Mechanism B should, however, not depend on changes of 'environmental' conditions. In this context it should be mentioned that the H^+ stoichiometry concluded above from the electrochromic changes is independent of the use of PS II membranes, PS II antenna particles or PS II core complexes, and independent of stronger treatment of the PS II, e.g., with the reducing agents such as HA and HH up to the S_{-2} state (Figs. 2 and 4). This result is different from the antenna dependent H^+ release behavior measured recently with pH indicators in Ref. 62 with thylakoids from pea.

Possible states of water

The estimated stoichiometry of the deprotonations is the basis of information on the water derivatives in the different S states. The water derivatives are, however, only available if at least the derivative for one S state is known. Such a 'calibration' becomes again possible if – as in the case of estimation of the Mn valences – use is made of results including the range of the over-reduced states. In the following we neglected at pH 7 the relatively small deviations from the integer values. The integer values of the H^+ release (−2: −1:0: −1), occurring with the $S_{-1} \rightarrow S_0 \rightarrow S_1 \rightarrow S_2 \rightarrow S_3$ transition at pH 7, are supposed to represent only the deprotonation of water ligated with the Mn complex (see last section).

In toto, 4 protons are released in the S_{-1}-S_3 transition. This is possible if 2 neutral H_2O molecules are located in S_{-1} (2 H_2O). Consequently, it must be S_0(2 OH^-), i.e., under physiological conditions water 'slips' into the cycle with the release of 2 protons. From EPR measurements, Andreasson et al. also concluded that there are 2 OH^- located in S_0 [54]. S_{-2} may be 'uncharged' and may contain therefore also 2 H_2O; this is, however, not measurable because of the first flash artefact and is indicated by the dotted circle in Fig. 9, bottom).

Since Mn oxidation takes place throughout the entire S-state transitions, water remains unoxidized up to S_3. That water is oxidized only in the S_3-S_4-S_0 transition is in concordance with the result that water $H_2^{18}O$ can still be replaced by $H_2^{16}O$ in the S_3 state [55,56]. With this information, consequently, the water derivatives in S_0-S_3 are available on the basis of the calibrated S_{-1}(2 H_2O) state together with the discussed H^+ stoichiometry. The result is shown in Fig. 9, bottom. The suggested derivatives may remain exchangeable with the water of the solvent.

This scheme is in agreement with other results: (1) The complete depletion of all protons prior to the $S_3 \rightarrow S_0$ transition is in line with energetic considerations which indicate that deprotonated water is the most favorable state for water oxidation in the $S_3 \rightarrow S_4 \rightarrow S_0$ transition [57]. (2) The absence of H^+ release with $S_1 \rightarrow S_2$ transition is in accordance with the observation that around pH 7 the $S_1 \rightarrow S_2$ transition is possible, even at 135 K, in contrast to all other transitions Refs. 58,59. This is understandable if at the catalytic site in this transfer deprotonation from water does not take place. (3) If according to the latter two points 4 H^+ are released prior to the $S_3 \rightarrow S_0$ transition and no H^+ is released with the $S_1 \rightarrow S_2$ transition, this is possible if 2 OH^- are located in S_0.

That in the $S_2 \rightarrow S_3$ transition protonation takes place, not from water but by oxidation of an amino-acid residue in the $S_2 \rightarrow S_3$ transition, coupled with the formation of an OH adduct on an imidazol ring as discussed in Ref. 53, is unlikely because besides the optical difference spectra (see above) recently it was shown also by the K-edge shift [45] that this transition is due to Mn oxidation (see above).

Very likely Mn is the binding site for water. The alternate oxidations of the first and second Mn ions in Fig. 9, top, render them useful as binding site for two water molecules. The function of the third redox-active Mn (in brackets) may be to trigger the O_2 evolution by

an inductive effect, if it is oxidized in the $S_3 \rightarrow S_4$ transition from Mn(III) to Mn(IV). Its increased positive charge in S_4 could make the oxidation potential of the Mn ions ligated with 2 O^{2-} sufficiently positive for an electron transfer from the oxo-atoms to these Mn ions [11]. As a precursor of the double bond of the O_2 formation a peroxo-intermediate may be considered. The evaluated water derivatives may be bound as terminal ligands at the Mn ions or may be integrated as bridges between two Mn ions. A scheme in which the two cycles in Fig. 9 from S_0 to S_4 are combined by terminal ligation of the derivatives of water with the three redox active Mn ions is shown in Ref. 61.

Acknowledgements

We are very grateful to Dr. Schlodder for his helpful critical comments. We thank D. DiFiore and C. Otto for the preparation of the PS II complexes, G. Baude for his excellent assistance in the MS measurements and Schering AG for making the MS equipment available for our investigations. The financial support from the Deutsche Forschungsgemeinschaft (Sfb 312) is gratefully acknowledged.

References

1 Junge, W. and Witt, H.T. (1968) Z. Naturforsch. 23b, 244–254.
2 Döring, G., Stiehl, H.H. and Witt, H.T. (1967) Z. Naturforsch. 22b, 639–644.
3 Döring, G., Renger, G., Vater, J. and Witt, H.T. (1969) Z. Naturforsch. 24b, 132–139.
4 Stiehl, H.H. and Witt, H.T. (1968) Z. Naturforsch. 23b, 1588–1598.
5 Debus, R.J., Barry, B.A., Babcock, G.T. and McIntosh, C. (1987) Proc. Natl. Acad. Sci. USA 85, 427–430.
6 Vermaas, W.F.J., Rutherford, A.W. and Hansson, Ö. (1988) Proc. Natl. Acad. Sci. USA 85, 8477–8481.
7 Gerken, S., Brettel, K., Schlodder, E. and Witt, H.T. (1988) FEBS Lett. 237, 69–75.
8 Kok, B., Forbush, B. and McGloin, M. (1970) Photochem. Photobiol. 11, 457–475.
9 Joliot, P., Barbieri, G. and Chabaud, R. (1969) Photochem. Photobiol. 10, 309–329.
10 Dekker, J.P., Van Gorkom, H.J, Wensink, J. and Ouwehand, L. (1984) Biochim. Biophys. Acta 767, 1–9.
11 Saygin, Ö. and Witt, H.T. (1987) Biochim. Biophys. Acta 893, 452–469.
12 Lavergne, J. (1989) Photobiochem. Photobiol. 50, 235–241.
13 Saygin, Ö. and Witt, H.T. (1984) FEBS Lett. 176, 83–87.
14 Saygin, Ö. and Witt, H.T. (1985) FEBS Lett. 187, 224–226.
15 Brettel, K., Schlodder, E. and Witt, H.T. ((1984) Biochim. Biophys. Acta 766, 403–415.
16 Bouges, B. (1971) Biochim. Biophys. Acta 234, 103–112.
17 Kok, B. and Velthuys, B.R. (1977) in Research in Photobiology (A. Castellani, ed.), pp. 111–119, Plenum Press, New York.
18 Saygin, Ö. and Witt, H.T. (1985) Photobiochem. Photobiophys. 10, 71–82.
19 Förster, V. and Junge, W. (1986) Photosyn. Res. 9, 197–210.
20 Radmer, R. and Ollinger, O. (1982) FEBS Lett. 144, 162–166.
21 Renger, G., Messinger, J. and Hanssum, B. (1990) in Current Research in Photosynthesis, Vol. 1 (Baltscheffsky, M., ed.), pp. 845–848, Kluwer, Dordrecht.
22 Beck, W.F. and Brudvig, G.W. (1987) Biochemistry 26, 8285, 82–95.
23 Kretschmann, H., Pauly, S. and Witt, H.T. (1991) Biochim. Biophys. Acta 1059, 208–214.
24 Messinger, J., Pauly, S. and Witt, H.T. (1991) Z. Naturforsch. 4c, 1033–1037.
25 Messinger, J. Wacker, U. and Renger, G. (1991) Biochem. 30, 7852–7862.
26 Schatz, G.H. and Witt, H.T. (1984) Photobiochem. Photobiophys. 7, 1–14.
27 Rögner, M., Dekker, J.P., Boekema, E.J. and Witt, H.T. (1987) FEBS Lett. 219, 207–211.
28 Kretschmann, H. (1992) Ph.D. Thesis, TU Berlin.
29 Van Gorkom, H.J., Van Leeuwen, J.P., Vos, M.H., Barends, J.P.F. (1990) Curr. Res. Photosynth. 1, 693–700.
30 Radmer, R. (1979) Biochim. Biophys. Acta 546, 418–425.
31 Renger, G., Bader, K.P. and Schmid, G.H. (1990) Biochim. Biophys. Acta 1010, 288–294.
32 He, P., Bader, K.P. and Schmid, G.H. (1991) Z. Naturforsch. 46c, 629–634.
33 Wieghardt, K., Bossek, U., Nuber, B., Weiss, J., Bonvoisin, J., Corbella, M., Vitols, S.E. and Girerd, J.J. (1986) J. Am. Chem. Soc. 110, 7398–7411.
34 Sivaraja, M. and Dismukes, G.C. (1988) Biochemistry 27, 6297–6306.
35 Tamura, N. and Cheniae, G.M. (1985) Biochim. Biophys. Acta 809, 245–259.
36 Styring, S. and Rutherford, A.W. (1987) Biochemistry 26, 2401–2405.
37 Stiehl, H.H. and Witt, H.T. (1969) Z. Naturforsch. 24b, 1588–1598.
38 Vermaas, W.F.J., Renger, G. and Dohnt, G. (1984) Biochim. Biophys. Acta 764, 194–202.
39 Mei, R. and Yocum, C.F. (1991) Biochemistry 30, 7836–7841.
40 Mei, R. and Yocum, C.F. (1992) Biochemistry 31, 8449–8454.
41 Kretschmann, H., Dekker, J.P., Saygin, Ö. and Witt, H.T. (1988) Biochim. Biophys. Acta 932, 358–361.
42 Van Leeuwen, P.J., Heimann, C., Dekker, J.P., Gast, P. and Van Gorkom, H.J. (1992) Res. Photosynth. 2, 325–328.
43 Lavergne, J. (1991) Biochim. Biophys. Acta 1060, 175–188.
44 Sauer, K., Guiles, R.D., McDermott, A.E., Cole, J.L., Yachandra, V.K., Zimmermann, J.-L., Klein, M.P., Dexheimer, S.L. and Britt, R.D. (1988) Chim. Scr. 28A, 87–91.
45 Ono, T., Noguchi, T., Inoue, Y., Kusunoki, M., Matsuhita, T., and Oyanagi, H. (1992) Science 258, 1335–1337.
46 Guiles, R.D., Yachandra, V.K., McDermott, A.E., Cole, J.L., Dexheimer, S.L., Britt, R.D., Sauer, K. and Klein, M.P. (1990) Biochemistry 29, 486–496.
47 Riggs, P.J., Mei, R., Yocum, C.F. and Penner-Hahn, J.E. (1992) J. Am. Chem. Soc. 114, 10650–10651.
48 Yachandra, V.K., Guiles, R.D., McDermott, A.E., Cole, J.L., Britt, R.D., Dexheimer, S.L., Sauer, K. and Klein, M.P. (1987) Biochemistry 26, 5974- 5981.
49 Yeh, S., Bayburt, T.H. and Sharp, R.R. (1990) Curr. Res. Photosynth. 1, 821–824.
50 Srinivasan, A.N. and Sharp, R.R. (1986) Biochim. Biophys. Acta 851, 369–376.
51 Pauly, S. and Witt, H.T. (1992) Biochim. Biophys. Acta 1099, 211–218.
52 Saphon, S. and Crofts, A. (1977) Z. Naturforsch. 32c, 617.
53 Rapapport, F. and Lavergne, J. (1991) Biochemistry 30, 1004–10012.
54 Andréasson, L.-E., Hansson, Ö. and Vänngard, T. (1983) Chim. Scr. 21, 1–74.

55 Radmer, R. and Ollinger, O. (1986) FEBS Lett. 195, 285–289.
56 Bader, K.P., Thibault, P. and Schmid, G.H. (1987) Biochim. Biophys. Acta 893, 564–571.
57 Krishtalik, L.I. (1990) Bioelectrochem. Bioenerg. 23, 249–263.
58 Koike, H. and Inoue, Y. (1987) in Progress in Photosynthesis Research, Vol. I (Biggins, J., ed.), pp. 645–648, Martinus Nijhoff, Dordrecht.
59 Styring, S. and Rutherford, A.W. (1988) Biochim. Biophys. Acta 983, 378–387.
60 Styring, S. and Rutherford, A.W. (1988) Biochemistry 27, 4915–4923.
61 Witt, H.T. (1991) Photosynth. Res. 29, 55–77.
62 Jahns, P. and Junge, W. (1992) Biochemistry 31, 7398–7403
63 Meyer, B., Schlodder, E., Dekker, J.P. and Witt, H.T. (1989) Biochim. Biophys. Acta 974, 36–43.